Semiclassical theory of the effects of collisions between rotors on molecular spectral line shapes. II. Calculations for several systems

Alexander F. Turfa,[a] Wing-ki Liu,[b] and R. A. Marcus

Department of Chemistry, University of Illinois, Urbana, Illinois 61801
(Received 29 March 1977)

The T_2 (microwave line broadening) and T_1 (microwave transient experiments) collisional cross sections are obtained by Monte Carlo trajectory evaluations of semiclassical (WKB) expressions for those quantities derived in a previous paper in this series. The calculated values of the cross sections presented here yields the relation $T_1 \approx T_2$ (within standard error) for the systems OCS–OCS, OCS–N_2, OCS–H_2, OCS–CO_2, and HCN–HCN, a result which agrees with recent experimental findings. Reasonable agreement was also found between the calculated values of the T_2 cross section and those observed spectroscopically.

I. RELAXATION TIMES

A. Expression for T_2 relaxation time

In a previous publication,[1] referred to as Paper I, a semiclassical expression was developed for the cross section describing the microwave line broadening phenomenon for two rigid rotors. In the present paper, the results of Paper I are used to compute T_1 and T_2 cross sections for several collision systems. Comparison of the calculated results is made with experimental data and with other results.[2,3] The numerous experimental and theoretical investigations in the field of microwave line broadening have been discussed in several comprehensive review articles.[4] Reference will also be made to previous applications of semiclassical dynamical theory to this field by Fitz and Marcus,[5] and by Liu and Marcus,[6] of which the present work is, in part, an extension.

For convenience and brevity, a glossary of symbols used in this paper is given in Table I, and a list of molecular parameters used in the calculations in Table II.

Collisions between two rigid rotors were treated semiclassically by Liu and Marcus,[6b] who assumed that the perturbing rotor could be approximated as a structureless (atomlike) particle. This assumption was reasonable in the case of the nonpolar rotors in Ref. 6(b) (as comparison with the present results shows), but in other cases, especially where a dipole–dipole interaction is important, the structureless approximation cannot be made, and it becomes necessary to take into account the full collision dynamics of two rotors.

In Paper I, a cross section, denoted by σ_{f_i,f_f}, was first obtained for a given relative velocity of the collision partners for the broadening of a spectral line $j_i \to j_f$. One can define a velocity-averaged cross section, $\bar{\sigma}$, given as

$$\bar{\sigma} = \langle v\sigma_{f_i,f_f}\rangle / \langle v\rangle , \tag{1.1}$$

where $\langle\ \rangle$ indicates a Maxwell–Boltzmann average over the relative velocity v. The quantity commonly measured in pressure-broadening experiments is the linewidth parameter Λ, in units of frequency per unit pressure. It is simply related to $\bar{\sigma}$[7]:

TABLE I. Glossary of symbols.

a	as a subscript, refers to the absorbing molecule.
p	as a subscript, refers to the perturbing molecule.
$\alpha^{\parallel}$, $\alpha^{\perp}$	are the parallel and perpendicular components of the diagonalized polarizability tensor that characterizes a linear (or symmetric top) molecule.
$\bar{\alpha}$	equals $(\alpha^{\parallel}+2\alpha^{\perp})/3$.
$\Delta\alpha$	as defined for linear molecules and symmetric tops, equals $\alpha^{\parallel}-\alpha^{\perp}$.
ϵ, σ	are the familiar parameters for the Lennard-Jones (12–6) potential.
σ	also denotes a cross section (no confusion is likely to arise).
$\bar{\sigma}$	is the velocity-averaged cross section.
R	is the distance between the centers of mass of the collision partners.
R_0	is the value of R at which the numerical integration of the trajectories is begun.
ψ, γ, γ_p	are the three angles describing the relative orientation of the two linear rotors, as depicted in Fig. 1 of Paper I.
n	is the gas density in molecules per volume and per torr.
$\bar{v}$	is the average relative velocity of the collision partners.
$\hat{j}$	is the semiclassical rotational angular momentum which equals $j+1/2$ where j is the quantum number, $\hat{l}$, $\hat{j}_p$, $\hat{h}$, and $\hat{J}$ are similarly defined.
$\bar{q}$	are the angle variables that are constants of the unperturbed motion and are conjugate to angular momenta.
q	are angle variables that increase linearly in time.
$\sum_{\text{s.p.}}$	is a sum over all stationary phase points that contribute to a particular expression.

[a] Present address: Huygens Laboratorium der Rijksuniversiteit te Leiden, Leiden, The Netherlands.

[b] Presend address: Department of Chemistry, University of Waterloo, Waterloo, Ontario, Canada.

TABLE II. Molecular parameters.

	$\alpha^{\parallel}$ (Å^3)	$\alpha^{\perp}$ (Å^3)	μ (D)	B (cm^{-1})	ϵ/k (°K)	σ (Å)
HCN	3.92[a]	1.92[a]	3.00	1.4784[b]	569.10[c]	3.63[c]
OCS	8.7[d]	4.0[d]	0.709	0.20286[e]	335[f]	4.13[f]
CO_2	3.94[g]	1.91[g]	0	0.3895[b]	189[f]	4.486[f]
N_2	2.22[g]	1.53[g]	0	2.010[h]	47.6[f]	3.85[f]
H_2	1.006[g]	0.7033[g]	0	60.80[h]	37.0[f]	2.928[f]

[a]Landolt-Börnstein, *Zahlenwerte und Funktionen* (Springer, Berlin, 1950), Band I, Teil 3, p. 510.
[b]G. Herzberg, *Infrared and Raman Spectra of Polyatomic Molecules* (Van Nostrand, New York, 1945).
[c]R. C. Reid and T. K. Sherwood, *The Properties of Gases and Liquids* (McGraw-Hill, New York, 1966), 2nd ed.
[d]S. A. Marshall and J. Weber, Phys. Rev. **105**, 1502 (1957).
[e]W. Gordy, W. V. Smith, and R. F. Trambarulo, *Microwave Spectroscopy* (Dover, New York, 1953).
[f]J. O. Hirschfelder, C. F. Curtiss, and R. B. Bird, *Molecular of Theory Gases and Liquids* (Wiley, New York, 1967).
[g]N. J. Bridge and A. D. Buckingham, Proc. R. Soc. London Ser. A **295**, 334 (1966). Whenever feasible, we have corrected the α's reported in this reference for optical dispersion.
[h]G. Herzberg, *Spectra of Diatomic Molecules* (Van Nostrand, New York, 1950), 2nd ed.

$$\Lambda = n\langle v\sigma_{fi,fi}\rangle/2\pi = n\langle v\sigma\rangle/2\pi\,. \tag{1.2}$$

For the sake of uniformity, all results from other sources, theoretical and experimental, have been converted from linewidths to cross sections for comparison in this paper.

In the bulk of the literature,[3,4,7] Λ is expressed in units of MHz Torr^{-1} and then $2\pi\Lambda p = 1/T_2$, where p is the pressure of the perturbing gas. No confusion should occur with the use of the symbol Λ as a relaxation matrix element in previous papers in this series[6] and in Eq. (1.10), to be given shortly.

Equation (4.9) of Paper I gives $\sigma_{fi,fi}$ and then, by Eq. (1.1), $\bar{\sigma}$ is obtained

$$\bar{\sigma} = 2\pi\int_0^\infty \bar{S}(b)b\,db\,, \tag{1.3}$$

where

$$\bar{S}(b) = \int_0^\infty dv 4\pi v^3\rho_v \int_0^\infty d\hat{j}_p\rho_{j_p}\int_{|\hat{j}_p-\hat{l}|}^{\hat{j}_p+\hat{l}} d\hat{h}(\hat{h}/2\hat{l}\hat{j}_p) \times\int_{|\hat{h}-\hat{j}|}^{\hat{h}+\hat{j}} d\hat{j}(\hat{J}/2\hat{h}\hat{j})\int_0^{2\pi}(d\bar{q}_l/2\pi) \times\int_0^{2\pi}(d\bar{q}_h/2\pi)\int_0^{2\pi}(d\bar{q}_{j_p}/2\pi)(1-P')\,, \tag{1.4}$$

where P' is the probability of a $j\to j$ transition, modified by a reorientational and dephasing factor D^1_{11}, and is given by (1.5) for a classically allowed transition:

$$P' = \sum_{\text{s.p.}} \left|\partial\hat{j}'/\partial(\bar{q}_j/2\pi)\right|^{-1} D^1_{11}(\alpha\beta\gamma)\,. \tag{1.5}$$

Here, $\hat{j}$ is the absorbing molecule's angular momentum, $\hat{j}_p$ is that of the perturbing molecule, $\hat{l}$ is that of the orbital angular momentum, $\hat{h}$ is that of h, where $\mathbf{h} = \mathbf{j}_p + \mathbf{l}$, and $\hat{J}$ is the total angular momentum ($\mathbf{J} = \mathbf{j} + \mathbf{h} = \mathbf{j} + \mathbf{j}_p + \mathbf{l}$), $\hat{j}$, $\hat{j}_p$, $\hat{l}$, $\hat{h}$, and $\hat{J}$, are related semiclassically to the angular momentum quantum numbers [e.g., $\hat{j} = (j+\frac{1}{2})\hbar$]; ρ_v and ρ_f are Boltzmann distribution functions given in Ref. 18 or Part I, and α and γ are phase-shifting angles and β the angle or reorientation between j and j′ [Fig. 3 cf. Ref. 6(a)]. As in Paper I, primed quantities are postcollisional.

The $\bar{S}(b)$ in Eq. (1.4) is the usual collision "efficiency function,"[2,3] and is marked by a bar to indicate that it is, like $\bar{\sigma}$, a velocity-averaged quantity. In Ref. 18 of Part I, the eight integrations in the expression for $\bar{\sigma}$ are changed to obtain a form more convenient for Monte Carlo evaluation by introducing a parameter B. One finds (writing $\bar{\sigma}$ as $\bar{\sigma}_{T_2}$ since it also determines a lifetime T_2 in microwave transient experiments[6,8]),

$$\bar{\sigma}_{T_2} = \int_0^1\cdots\int_0^1 (\pi B^2/x_b)(1-P'_{\hat{j},\hat{j}})\,d\mathbf{x}\,, \tag{1.6}$$

where the x variables are defined in Ref. 18 of Part I and where

$$d\mathbf{x} = dx_{q_p}\,dx_{a_l}\,dx_{q_h}\,dx_{j_p}\,dx_h\,dx_J\,dx_v\,dx_b\,. \tag{1.7}$$

In the "primitive semiclassical approximation," $P'_{\hat{j},\hat{j}}$ for classically allowed trajectories is

$$P'_{\hat{j},\hat{j}} = \text{Re}\sum_{\text{s.p.}} \left|\partial\hat{j}'/\partial(\bar{q}_j/2\pi)\right|^{-1} D^1_{11}(\alpha\beta\gamma)\,, \tag{1.8}$$

where Re denotes "the real part of." The sum $\sum_{\text{s.p.}}$ is over all trajectories (real or complex valued) leading from state $\hat{j}$ of the absorbing rotor to the same postcollisional state $\hat{j}'(=\hat{j})$. The semiclassical action $\hat{j}$ is the average of $\hat{j}_i$ and $\hat{j}_f$ and thereby, in units of $\hbar = 1$ used in this paper,

$$\hat{j} = \tfrac{1}{2}(j_i + j_f) + \tfrac{1}{2}\,, \tag{1.9}$$

where the radiative transition of the absorbing molecule is between the two quantum states: $i\to f$. In the microwave dipole absorption spectrum, $j_f = j_i + 1$.

When the problem has additional symmetry [symmetry in the intermolecular potential with respect to some or all of the $\bar{q}$ variables in Eq. (1.4)], interferences occur and Eq. (1.8) is replaced by

$$P'_{\hat{j},\hat{j}'} = \text{Re}\,s\sum_{\text{s.p.}} \left|\partial\hat{j}'/\partial(\bar{q}_j/2\pi)\right|^{-1} D^1_{11}(\alpha\beta\gamma)\,. \tag{1.10}$$

In such a case, the integration region in Eq. (1.4) is appropriately reduced. The significance of the symmetry number s, the value of which determines this reduced region of $(\bar{q}_j, \bar{q}_l, \bar{q}_{j_p}, \bar{q}_h)$ space implied in Eqs. (1.8) and (1.10) to be searched for stationary phase points, is explained in greater detail in Appendix A.

B. Expression for T_1 relaxation time

In addition to the measurements of line broadening relaxation times (commonly designated as T_2) a relaxation time T_1, associated with equilibrium in the population of the levels of a two-state system, has also been measured recently.[8] The cross section described by Eqs. (1.2) and (1.3) is $\bar{\sigma}_{T_2}$, while now a similar expression for $\bar{\sigma}_{T_1}$ is discussed.

By Eq. (3.12) of Liu and Marcus,[6b]

$$\frac{1}{T_1} = \tfrac{1}{2}(\Lambda_{ii,ii} - \Lambda_{ff,ii} + \Lambda_{ff,ff} - \Lambda_{ii,ff}) . \tag{1.11}$$

Equation (2.2) of Ref. 6(a) gives the Λ in terms of S-matrix elements, which when combined gives for the rhs of Eq. (1.11):

$$\tfrac{1}{2}(1 - |S_{ii}|^2 + 1 - |S_{ff}|^2 + |S_{if}|^2 + |S_{fi}|^2)$$
$$= \tfrac{1}{2}(2 - P_{ii} - P_{ff} + P_{if} + P_{fi}) . \tag{1.12}$$

This expression can be simplified as follows: since $P_{if} = P_{fi}$ and since it is a good approximation to replace P_{ii} and P_{ff} each by a mean valued $P_{\hat{j},\hat{j}}$, where $\hat{j}$ is defined by Eq. (1.9), and approximate P_{if} by $P_{\hat{j},\hat{j}+1}$; similarly, one obtains

$$\bar{\sigma}_{T_1} = \int_0^1 \cdots \int_0^1 (\pi B^2/x_b)(1 - P_{\hat{j},\hat{j}} + P_{\hat{j},\hat{j}+1})\, d\mathbf{x} , \tag{1.13}$$

where $d\mathbf{x}$ is given by Eq. (1.7).

In the "primitive semiclassical approximation," the P's, vis-à-vis the P''s in Eq. (1.8), are

$$P = \sum_{\text{s.p.}} |\partial \hat{j}'/\partial(\bar{q}_j/2\pi)|^{-1} , \tag{1.14}$$

[or multiplied by $\exp(-2\Phi)$ when the trajectory is complex valued[1,5a]]. In the case of additional symmetry already mentioned in Sec. I.A, Eq. (1.14) is replaced by

$$P = s \sum_{\text{s.p.}} |\partial \hat{j}'/\partial(\bar{q}_j/2\pi)|^{-1} , \tag{1.15}$$

where the symmetry number s and the reduced integration region are discussed in Appendix A.

The derivative is evaluated with trajectories leading from $\hat{j}$ to $\hat{j}$ or to $\hat{j}+1$, as indicated by the subscripts on the P's, and the sum is over all such trajectories. In $\bar{\sigma}_{T_1}$, there exist no effects of phase shifting or reorientation as are present in $\bar{\sigma}_{T_1}$ via the rotation matrix element $D^1_{11}(\alpha\beta\gamma)$ in Eq. (1.8). Thus one has in Eq. (1.13) an integrand which is evaluated by the Monte Carlo method for choosing precollisional values of dynamical variables and by varying $\bar{q}_j$ systematically to locate numerically real or complex-valued stationary phase points such that $\hat{j}' = \hat{j}$ (or $\hat{j}+1$, for $P_{\hat{j},\hat{j}+1}$). In Eq. (1.8) for $\bar{\sigma}_{T_2}$, one needs only the plot of $\hat{j}'$ vs $\bar{q}_j$ for $\hat{j}' = \hat{j}$.

Upon comparing the integrands for the $\bar{\sigma}_{T_1}$ and $\bar{\sigma}_{T_2}$ expressions, one would expect these two cross sections to be approximately equal whenever a $\hat{j} \to \hat{j}+1$ *collisional* transition is either strictly forbidden, as it is for the nonpolar interaction potentials,[5,6] or when there are many readily accessible postcollisional states. [In either case, for $\bar{\sigma}_{T_1}$ to nearly equal $\bar{\sigma}_{T_2}$ it is necessary for $\mathrm{Re}D^1_{11}(\alpha\beta\gamma)$ to be almost unity, as is found to be the case in most collisions at 300 °K.][6b] Indeed, Liu and Marcus[6b] found $\bar{\sigma}_{T_1}$ and $\bar{\sigma}_{T_2}$ to be equal within 10% for the systems that they studied.

II. INTERMOLECULAR POTENTIALS

As already noted, Liu and Marcus[6b] treated the perturbing rotor as a structureless particle. A potential function for that model which includes a repulsive core and London dispersion interactions, with anisotropy in the latter is[9]

$$V(R,\gamma) = 4\epsilon\left[\left(\frac{\sigma}{R}\right)^{12} - \left(\frac{\sigma}{R}\right)^{6}[1 + a_p P_2(\cos\gamma)]\right] . \tag{2.1}$$

To obtain ϵ and σ for two nonidentical colliding molecules, the usual combining rules[10] are employed:

$$\epsilon = (\epsilon_a \epsilon_p)^{1/2} , \qquad \sigma = (\sigma_a + \sigma_b)/2 . \tag{2.2}$$

The anisotropy parameter a_p is given as[10]

$$a_p = \Delta\alpha_a / 3\bar{\alpha}_a , \tag{2.3}$$

where $\Delta\alpha$ and $\bar{\alpha}$ are defined in Table I; a_p depends *only* upon the properties of the absorbing rotor by this model. The potential which is analogous to Eq. (2.1) but which includes the full dynamics of two rotors is[4a]

$$V_{\text{disp}}(R,\gamma,\gamma_p,\psi) = [c_1(\cos\psi - 3\cos\gamma\cos\gamma_p)^2 + c_2\cos^2\gamma + c_3\cos^2\gamma_p + c_4]/R^6 , \tag{2.4}$$

where

$$c_1 = c'(\alpha_a^{\parallel} - \alpha_a^{\perp})(\alpha_p^{\parallel} - \alpha_p^{\perp})/3 , \tag{2.5a}$$

$$c_2 = c'(\alpha_a^{\parallel} - \alpha_a^{\perp})\alpha_p^{\perp} , \tag{2.5b}$$

$$c_3 = c'(\alpha_p^{\parallel} - \alpha_p^{\perp})\alpha_a^{\perp} , \tag{2.5c}$$

$$c_4 = c'(\bar{\alpha}_a\alpha_p^{\perp} + \bar{\alpha}_p\alpha_a^{\perp}) , \tag{2.5d}$$

where $\alpha^{\parallel}$ and $\alpha^{\perp}$ are defined in Table I and where

$$c' = -2\epsilon\sigma^6/(\bar{\alpha}_a\bar{\alpha}_p) . \tag{2.5e}$$

Actually, the potential previously used [in Refs. 3(a)–3(c) and in other references cited in Ref. 4(a)] did not have c' given by Eq. (2.5e), but instead

$$c' = -(3/4)I_a I_p/(I_a + I_p) , \tag{2.6}$$

where I_a and I_p are ionization potentials. This latter potential represents a weaker interaction than does Eq. (2.4). For example, c' by Eq. (2.5e) is about 1.8 times larger than the same quantitiy by Eq. (2.6) for OCS–N_2. The constant c' in Eq. (2.5e) was chosen as a clear extension of the form of Eq. (2.1).

The reduction of Eq. (2.4) to Eq. (2.1) is evident when isotropy of the perturber is assumed (i.e., $\bar{\alpha}_p = \alpha_p^{\parallel} = \alpha_p^{\perp}$, the rotor–atom model).

In this paper, Eq. (2.4) is used, plus the repulsion term $4\epsilon(\sigma/R)^{12}$ for the intermolecular potential. When both the perturber and absorber have permanent dipole moments, the dipole–dipole Hamiltonian [e.g., Ref. 4(a)]

$$H_{dd} = \mu_a\mu_p(\cos\psi - 3\cos\gamma\cos\gamma_p)/R^3 \tag{2.7}$$

is included.

III. METHOD OF CALCULATION

The T_2 cross section given by Eq. (1.6) and the T_1 cross section given by Eq. (1.13) were computed. The real and imaginary parts of the former give, respectively, the width and the frequency shift of the spectral peak.

For a particular collision system, the integrands of Eqs. (1.6) and (1.13) were calculated by assigning val-

ues to the eight x variables there, and evaluating the integrals by the Monte Carlo method. After the initial conditions were chosen at random, the classical equations of motion were solved numerically. By increasing $\bar{q}_j$, the precollisional barred angle variable conjugate to $\hat{j}$, in increments of $\pi/12$, a grid of the postcollisional semiclassical action of the absorbing rotor, $\hat{j}'$, was generated numerically as a function of $\bar{q}_j$ for each set of the eight x variables.

When real stationary phase points occurred (i.e., when there were real values of $\bar{q}_j$ for which $\hat{j}'$ equals $\hat{j}$), the $|\partial\hat{j}'/\partial\bar{q}_j|$ appearing in Eqs. (1.6) and (1.13) was evaluated at each such real stationary phase point of which there were usually two or four. The contributions to the calculated results are simply additive as indicated by the sum over stationary phase points $\sum_{s.p.}$ in these same equations. The rotation matrix element $D^1_{11}(\alpha\beta\gamma)$ that includes the effects of phase shifting and reorientation was also evaluated for use in Eq. (1.6). If there were no real stationary phase points, a parabola was fitted through the highest (or lowest) three points in the $\hat{j}'$ vs $\bar{q}_j$ grid. When this curve failed to cross the value $\hat{j}$, the computer program searched for points of closest approach to this value. If none were found within one action unit, the elastic probability $P^l_{\hat{j},\hat{j}}$ was taken as zero. If the curve had a point of closest approach within one action unit of $\hat{j}$, the familiar Airy function theory[11,12] was used to treat the two complex conjugate values of $\bar{q}_j$ that are roots (stationary phase points) to the $\hat{j}'$ vs $\bar{q}_j$ plot analytically continued into the complex plane. In such cases, the $\sum_{s.p.}|\partial\hat{j}'/\partial\bar{q}_j|^{-1}$ appearing in Eqs. (1.8) and (1.14) was replaced by $(\pi/2)|\partial\hat{j}'/\partial\bar{q}_j|^{-1}\rho^{1/2}\,\mathrm{Ai}^2(\rho)$, where $(4/3)\rho^{3/2}$ equals $\mathrm{Im}[\Delta(\bar{q}_c)-\Delta(\bar{q}_c^*)]$, for a complex root $\bar{q}_c$. The function Δ has been explained in detail elsewhere.[5,6]

The value of the symmetry number is determined by the symmetry properties of the intermolecular potential. When the anisotropy of the potential function is confined to even Legendre polynomials $P_{2n}(\cos\gamma)$ (e.g., the rotor–atom model), $\bar{q}_j$ and $\bar{q}_j+\pi$ result in identical collision dynamics and the $\hat{j}'$ vs $\bar{q}_j$ grid need be calculated only over the $[0,\pi]$ interval. In Appendix A, it is shown that these conditions, which result in $s=4$, hold also for the dispersion interaction in the rotor–rotor system in Eq. (2.4). In such cases, interference effects result in the collisional selection rule: $\Delta\hat{j}'=\hat{j}-\hat{j}'=0,\pm2$, etc., and the $P_{\hat{j},\hat{j}+1}$ in Eq. (1.13) is identically zero.

For the polar systems, HCN–HCN and OCS–OCS, the inclusion of the dipole–dipole term, Eq. (2.7) introduced a $P_1(\cos\gamma)$ dependence, and the potential is not invariant when $\bar{q}_j$ is increased by π. This necessitates computing the $\hat{j}'$ value over a $\bar{q}_j$ interval of $[0,2\pi]$, and s is found in Appendix A to equal 1.

The relatively weak dipole–dipole forces for OCS–OCS were found to result in near symmetries for many trajectories. In this case, the grid for the system was taken over the $\bar{q}_j$ interval of $[0,2\pi]$, and the symmetry number, s equal to 2. (This way would be used also to treat nonpolar systems having $\Delta\hat{j}=0,\pm2$ if the grid were increased to $[0,2\pi]$.) Both the formal inclusion of the partially symmetry-breaking dipole–dipole forces and the numerically resulting near symmetries and the concommitant interference effects were approximately taken into account in this manner.

The $\bar{q}$ variables appearing in Eq. (1.4) and which were chosen at random as initial conditions are constants of the two rotors' motion in the absence of intermolecular interaction. They are canonically conjugate to the precollisional angular momenta and are simply related to the more familiar q variables (which vary linearly with time in the absence of interaction), as in Ref. 18 of Part I.

For computational purposes, a collision trajectory was begun with an initial value of the intermolecular separation R set equal to the value R_0. At this point conversion to the unbarred angle variables was made using Eq. (B12) of Ref. 18 of Part I and then, as discussed elsewhere in that reference, to Cartesian coordinates in order to integrate Hamilton's equations numerically. (Alternatively, integration in action–angle variables could have been performed.) When the postcollisional separation R' again equals R_0, all of the postcollisional values of the dynamical variables have been computed, particularly $\hat{j}'$. The criterion for choosing R_0 for each system studied was that, at R_0, the maximum intermolecular potential energy be less than 1% of the average relative kinetic energy at 300 °K. The actual values of R_0 used for the systems listed in Table III were, respectively, 25, 35, 35, 50, and 120 a.u.

One hundred points were selected for the Monte Carlo averaging over the eight x variables, and a $\hat{j}'$ vs $\bar{q}_j$ grid was generated for each point of integration. The standard error, δ, associated with the Monte Carlo evaluation of each cross section is given by[6b,13]

$$\delta^2=\sum_{i=1}^{n}(\bar{\sigma}_i-\bar{\sigma})^2/n(n-1), \tag{3.1}$$

where $\bar{\sigma}$ equals either $\bar{\sigma}_{T_1}$ or $\bar{\sigma}_{T_2}$, and $\bar{\sigma}_i$ the contribution to that quantity from an individual point of Monte Carlo integration. The interval $[\bar{\sigma}-\delta,\ \bar{\sigma}+\delta]$ is, therefore, the "68% confidence interval."[13] Extending the interval to $[\bar{\sigma}-2\delta,\ \bar{\sigma}+2\delta]$ increases the confidence to 95%. In this paper, results are reported with standard error $\pm\delta$.

In generating the $\hat{j}'$ vs $\bar{q}_j$ grid, it was observed that in nearly every trajectory the intermolecular distance R decreased monotonically to a minimum value and then monotonically increased. Deviations from such behavior are examples of orbiting motion or of the formation of complexes during the collision. Since orbiting occurs only for low kinetic energy, it may be assumed that the contribution from orbiting resonances to the energy-averaged cross sections at room temperature is small. For the nonpolar systems OCS–N_2 and OCS–CO_2, such trajectories did occur, and those with more than five turning points in the R motion were rejected. The set of initial conditions that gave rise to these rejected trajectories were not included in calculating the averaged results, in order to reduce computer time. (Some trajectories evidenced 50 or more turning points.) Detailed examination of such trajectories revealed that grids

TABLE III. Results.

System	Transition	Cross sections (Å^2) $\bar{\sigma}_{T_1}$ (calc)	$\mathrm{Re}\bar{\sigma}_{T_2}$ (calc)	$\mathrm{Re}\bar{\sigma}_{T_2}$ (exptl)
OCS–H_2	1 → 2	41 ± 4	49 ± 4	65 ± 2[a]
OCS–N_2	1 → 2	113 ± 8	121 ± 8	149 ± 4[a]
OCS–CO_2	1 → 2	198 ± 16	205 ± 16	199 ± 5[a]
OCS–OCS	1 → 2	241 ± 24	227 ± 19	249 ± 2[b]
HCN–HCN	0 → 1	529 ± 62	598 ± 62	711 ± 228[c]

[a]Reference 7(a).
[b]An average of 243 ± 2 of Ref. 8(c) and 254 ± 2 of S. C. M. Luijendijk, Ph.D. dissertation, Utrecht, The Netherlands, 1973. In Ref. 8(c), $\bar{\sigma}_{T_1} = 234 \pm 13$ Å^2.
[c]A. G. Smith, W. Gordy, J. W. Simmons, and W. V. Smith, Phys. Rev. 75, 1524 (1949).

composed of $\hat{j}'$ values arising from trajectories with different numbers of turning points did not exhibit noticeable discontinuities. Furthermore, when such grids were compared with nonorbiting, non-complex-forming, grids generated from similar initial conditions (i.e., similar b and p_R), the occurrence or nonoccurrence of orbiting or complex-forming motion was seen to make very little difference in the contribution of such trajectories to the calculated results.

Thereby, 2% of all sets of initial conditions were rejected for OCS–N_2, 12% for OCS–CO_2, and none for OCS–H_2. For the polar systems, trajectories with more than 15 turning points were rejected, thereby leading to the omission of 13% of the sets of initial conditions for OCS–OCS and 11% for HCN–HCN. This general increase of incidence of orbiting and complex forming with strength of interaction is to be expected, but appears to play no important role in the present approximation in line broadening in the systems studied.[14]

When the $\hat{j}'$ vs $\bar{q}_j$ plot just barely intersects the desired postcollisional value of $\hat{j}'$, yielding stationary phase points so close to each other that interference occurs, a uniform approximation should replace the primitive semiclassical (PSC) value used in the present work. (Under such conditions the PSC value can exceed unity.) For simplicity, the term $\sum_{s.p.} |\partial \hat{j}'/\partial(\bar{q}_j/2\pi)|^{-1} D^1_{11}(\alpha\beta\gamma)$ was replaced by this quantity divided by $\sum_{s.p.} |\partial \hat{j}'/\partial(\bar{q}_j/2\pi)|^{-1}$ to avoid values exceeding unity. Better still might have been to simply replace it by unity in such cases (as in previous papers[6] of this series). Whichever of these two schemes of normalization of probabilities is chosen, the effect on the values of the T_1 and T_2 cross sections is negligible (that is, much smaller than the standard deviations in the calculated results).

The necessity of including complex stationary phase points in evaluating the probabilities, in the use of the Airy function as described earlier in this section, was found to be more frequent in computing the $P_{\hat{j},\hat{j}+1}$ term in the rhs of Eq. (1.13) than for computing $P_{\hat{j},\hat{j}}$, for the polar systems. Complex stationary phase points arising from points of closest approach within one action unit of the desired $\hat{j}'$ value occurred for 11% of all trajectories (for both $\bar{\sigma}_{T_1}$ and $\bar{\sigma}_{T_2}$) for OCS–CO_2, 18% for OCS–N_2, and only 1% for OCS–H_2. For $\bar{\sigma}_{T_2}$ in the polar systems, they occurred in 7% of all trajectories for OCS–OCS and 5% for HCN–HCN. For $\bar{\sigma}_{T_1}$, however, the frequency was 45% for OCS–OCS and 67% for HCN–HCN.

IV. RESULTS

The collision systems and spectral transitions of the absorbing molecules studied, together with the calculated T_1 and T_2 cross sections, are listed in Table III. The calculated results contain no adjustable parameters.

The computed values of the cross sections $\mathrm{Re}\bar{\sigma}_{T_2}$ and $\bar{\sigma}_{T_1}$ are relatively close to each other, which indicates little phase shifting and reorientation effect in the collisions. These values are also in reasonable agreement with experimental measurements of the T_2 linewidth, considering that the only anisotropic terms included in the intermolecular potential were the dispersion [Eq. (2.4)] and dipole–dipole [Eq. (2.7)] interactions. In general, the calculated cross sections were about 15% smaller than experimental values. In the case of small cross sections, one would also expect important contributions from short range (repulsive) anisotropies as well as from the attractive forces such as those arising from molecular quadrupole moments. The calculated frequency shifts, $\mathrm{Im}\bar{\sigma}_{T_2}$, are relatively small as is also found in experiment. They are scarcely larger than their standard deviations and are not given here. The Monte Carlo standard errors, δ, for $\mathrm{Re}\bar{\sigma}_{T_2}$ and for $\bar{\sigma}_{T_1}$ are about equal to, or smaller than, 10% of those values, which is a good indication of the general validity of the sampling techniques employed in these calculations.

Earlier, Liu and Marcus[6] had treated the OCS–N_2 system by approximating N_2 as a spherically averaged particle (an atom). For the 1 – 2 transition of OCS, their theory results in a T_2 linewidth of 118 ± 9 Å^2. This value compares well with the result in the present work, 121 ± 8 Å^2, obtained without this approximation.

It is difficult to make a meaningful comparison with previous theoretical work in the literature because of differences in the intermolecular potentials used. Most such calculations have been based on the Anderson theory[2] (linear trajectories, a perturbation treatment for rotational–translational collision dynamics, and a cutoff imposed at small impact parameters whenever the inelastic collisional probabilities exceeded unity), or via a related perturbation approach.[3] In the case of HCN–HCN, a calculation including only dipole–dipole forces has been reported by Murphy and Boggs.[3c] Their T_2 cross section is 597 Å^2, which is in agreement with the present result, 598 Å^2. Perturbation theory works well at large impact parameters, and with the aid of a cutoff or other approximation at smaller impact parameters appears to be quite satisfactory, at least in this example. However, if one attempted to calculate inelastic collisional probabilities for multiple quantum transitions, appreciable errors would be expected.

Molecular quadrupole moments have frequently been included in linewidth calculations.[3,4] In fact, these quadrupole moments have been calculated, via the Anderson theory and via another perturbation approach,[3c]

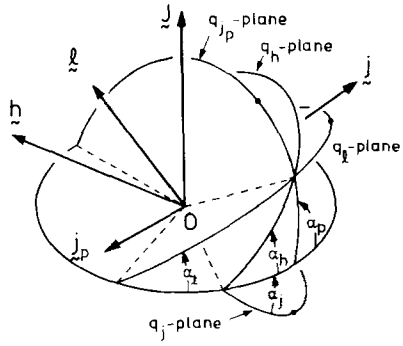

FIG. 1. Angular relations between the various planes of rotation associated with the angular momenta for use in examining symmetry properties of the intermolecular potential function in Appendix A. Cf. Fig. 5 of Ref. 18 of Paper I, where the $\hat{q}$'s are the present q's.

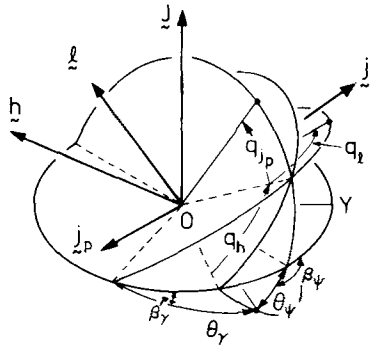

FIG. 3. Additional angles defined for use in Appendix A. Cf. Figs. 1 and 2.

by choosing values that result in optimum agreement between calculated linewidths and experiment. However, the product, $Q_{OCS} \cdot Q_X$, where X = OCS, CO_2, N_2, or H_2, that appears in the quadrupole–quadrupole interaction[3,4a] determined by this procedure is sometimes too high by factors ranging from 3 to 10 when compared with later actual measurements of Q for these molecules.[15] The quadrupole interactions evidently contribute relatively little to the linewidths when dipole–dipole and dispersion interactions are larger.

In summary, the calculations of the linewidths are in reasonable agreement with experimental results. The calculated T_1 and T_2 cross sections were found to be equal within standard error. It would be interesting to explore the contributions from shorter-range anisotropies to these and other cross sections, especially in systems where the long range anisotropies are relatively small.

APPENDIX A: SYMMETRY CONSIDERATIONS

The summation $\sum_{s.p.} |\partial j'/\partial(\bar{q}_j/2\pi)|^{-1}$ appearing in Eq. (1.5) has a simple interpretation as explained in Secs. I and III. In actual computations, however, use was made of symmetries of the two potential functions (with and without the dipole–dipole interactions) and the interferences arising from these symmetries to reduce the volume of $\bar{q}_j$, $\bar{q}_{j_p}$, $\bar{q}_h$, $\bar{q}_l$ space that is to be searched for stationary phase points. In order to consider this in detail, the potential functions are first examined, in particular their dependence on the angles $\bar{q}_l$, $\bar{q}_j$, $\bar{q}_{j_p}$, and $\bar{q}_h$ conjugate to the angular momenta $\hat{l}$, $\hat{j}$, $\hat{j}_p$, and $\hat{h}$.

Equations (2.4) and (2.7) give the potentials in terms of γ, γ_p, and ψ, and these angles are expressed in terms of the four q variables: The procedure is fundamentally straightforward but involves a large number of spherical trigonometric manipulations. The various rotational planes are depicted in Fig. 1, and various angles γ_p, q_{j_p}, q_l, etc., are defined in Fig. 2. One can rather easily show

$$\cos\gamma_p = \cos q_{j_p} \cos q_l + \sin q_{j_p} \sin q_l (\hat{h}^2 - \hat{l}^2 - \hat{j}_p^2)/(2\hat{l}\hat{j}_p) . \quad \text{(A1)}$$

Incidentally, the q's in the present paper were denoted by $\hat{q}$'s in Paper I, but the carets are now deleted for notational brevity.

Similar expressions for $\cos\gamma$ and $\cos\psi$ are obtained in a less direct manner. First, angles α_l, α_p, α_j, β_γ, β_ψ, θ_γ, and θ_ψ are defined as shown in Figs. 1 and 3. It is evident that $\cos\alpha_j = \hat{m}_j/\hat{j}$, $\cos\alpha_l = \hat{m}_l/\hat{l}$, $\cos\alpha_p = \hat{m}_p/\hat{j}_p$ and that the following relations hold:

$$\cos\theta_\gamma = -\cos D \cos q_j - \sin D \sin q_j \cos(\pi - \alpha_j) , \quad \text{(A2)}$$

and

$$\cos\beta_\gamma = (-\cos q_j - \cos\theta_\gamma \cos D)/(\sin\theta_\gamma \sin D) , \quad \text{(A3)}$$

where D, as well as A, B, C, and E, are defined in Fig. 4 and, analytically, in Ref. 18 of Part I. Next, one obtains

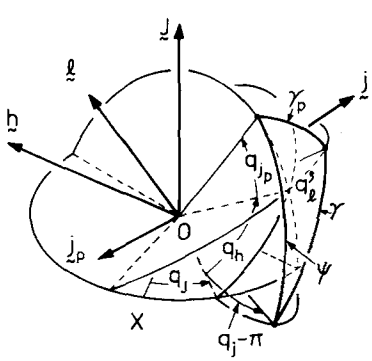

FIG. 2. Angles defined for use in Appendix A. Cf. Fig. 1.

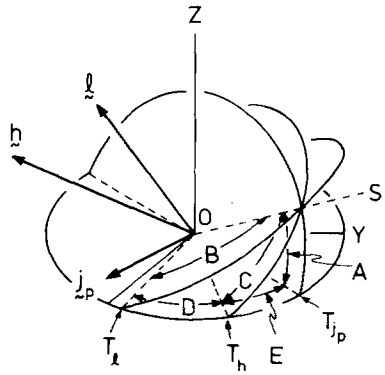

FIG. 4. Additional angles defined for use in Appendix A. Cf. Figs. 1–3.

$$\cos\gamma = \cos(q_l + B)\cos\theta_\gamma + \sin(q_l + B)\sin\theta_\gamma \cos(\alpha_l + \beta_\gamma)\,. \tag{A4}$$

Similarly, one finds

$$\cos\theta_\psi = -\cos q_j \cos E - \sin q_j \sin E \cos\alpha_j\,, \tag{A5}$$

$$\cos\beta_\psi = (\cos q_j + \cos\theta_\psi \cos E)/(\sin\theta_\psi \sin E)\,, \tag{A6}$$

and

$$\cos\psi = \cos(q_{j_p} + A)\cos\theta_\psi - \sin(q_{j_p} + A)\sin\theta_\psi \cos(\alpha_p + \beta_\psi)\,. \tag{A7}$$

Now, one notes that the substitution $q_j \to q_j - \pi$ results in $\theta_\gamma \to \theta_\gamma - \pi$, but that it leaves β_γ unchanged. Similarly, the substitution $q_j \to q_j - \pi$ results in $\theta_\psi \to \theta_\psi - \pi$ but β_ψ is unchanged. Also, it is evident that A, B, C, D, E, α_p, α_l, and α_j that determine the relative orientation of the planes of motion are not changed by such substitutions.

In the dispersion potential given by Eq. (2.4), one sees that the only term that needs to be inspected for symmetrical behavior for any or all of the substitutions,

$$q_l \to q_l - \pi\,, \quad q_j \to q_j - \pi\,, \quad q_{j_p} \to q_{j_p} - \pi\,, \tag{A8}$$

is the term which contains the product $\cos\gamma \cos\gamma_p \cos\psi$. One finds that this term, and hence the entire dispersion potential, is invariant under any one, and hence any two, or all three of the substitutions (A8).

Recalling from Paper I that $q_h = \bar{q}_h = C$, one finds that neither γ nor ψ, and hence no potential expressed in $\cos\gamma$ or $\cos\psi$, has a simple symmetry property when $\bar{q}_h (= C)$ is changed by π. This means that any search for stationary phase points must be conducted over the full $[0, 2\pi]$ interval of $\bar{q}_h$.

The $\bar{q}_j$, $\bar{q}_{j_p}$, $\bar{q}_l$ space is next considered as a cube with eight octants. Since the dispersion potential (e.g., OCS–N_2) is invariant under any or all of the substitutions Eq. (A8), all octants are equivalent and one can search the $\bar{q}_j$, $\bar{q}_{j_p}$, and $\bar{q}_l$ dimensions each in a $[0, \pi]$ interval for stationary phase points that contribute to an S-matrix element and then take the effect of interferences on $\bar{\sigma}$ from the eight octants into account. This method has been explained by Fitz and Marcus[5]: one considers the integral expression for an S-matrix element[11]

$$\langle \hat{j}_p' \hat{j}' \hat{l}' \hat{h}' | S^J | \hat{j}_p \hat{j} \hat{l} \hat{h} \rangle = \int_0^1 \int_0^1 \int_0^1 \int_0^1 |\partial(\bar{w}_j', \bar{w}_{j_p}', \bar{w}_l', \bar{w}_h')/\partial(\bar{w}_j \bar{w}_{j_p} \bar{w}_l \bar{w}_h)|^{-1/2} e^{i\Delta}\, d\bar{w}_j\, d\bar{w}_{j_p}\, d\bar{w}_l\, d\bar{w}_h\,, \tag{A9}$$

where

$$\Delta = \bar{q}_j(\bar{j} - \hat{j}') + \bar{q}_{j_p}(\bar{j}_p - \hat{j}_p') + \bar{q}_h(\bar{h} - \hat{h}') + \bar{q}_l(\bar{l} - \hat{l}') - \int_{p_R}^{\bar{p}_R} R\, dp_R - \int_{\hat{l}}^{\hat{l}'} q_l(t)\, d\hat{l}(t) - \int_{\hat{j}}^{\hat{j}'} q_j(t) d\hat{j}(t) - \int_{\hat{j}_p}^{\hat{j}_p'} q_{j_p}(t)\, d\hat{j}_p(t) - \int_{\hat{h}}^{\hat{h}'} q_h(t) d\hat{h}(t) + \tfrac{1}{2}\pi(\hat{l} + \hat{l}' + 1)\,. \tag{A10}$$

Applying the symmetry properties of Eq. (A8) to this expression, one obtains

$$\int_0^{2\pi} d\bar{q}_h \int_0^{2\pi} d\bar{q}_j \int_0^{2\pi} d\bar{q}_{j_p} \int_0^{2\pi} d\bar{q}_l = (1 + e^{i\pi(\hat{l} - \hat{l}')})(1 + e^{i\pi(\hat{j}_p - \hat{j}_p')})(1 + e^{i\pi(\hat{j} - \hat{j}')}) \int_0^{2\pi} d\bar{q}_h \int_0^{\pi} d\bar{q}_l \int_0^{\pi} d\bar{q}_j \int_0^{\pi} d\bar{q}_{j_p}\,. \tag{A11}$$

This expression thereby contains the selection rules that $(\hat{l} - \hat{l}')$, $(\hat{j} - \hat{j}')$, and $(\hat{j}_p - \hat{j}_p')$ must each be even. As a consequence, the S-matrix element for a particular $\hat{j} \to \hat{j}'$ elastic collision vanishes for $\frac{1}{2}$ of all the l' and also for $\frac{1}{2}$ of the $\hat{j}_p'$, and that for those values for which it does not vanish, one multiplies by 2^3, i.e., by 8, the contribution from one octant. The $\sum_{s.p.}$ in Eq. (1.5) implies that the root search is over $[0, 2\pi]$ for each $\bar{q}$ differential. When this is reduced to a $[0, \pi]$ interval for $\bar{q}_j$, $\bar{q}_{j_p}$, and $\bar{q}_l$, the integral is changed as follows (before the partial averaging discussed in Sec. IV of Paper I):

$$\int_0^\infty d\hat{J} \int_0^\infty d\hat{l}' \int_0^\infty d\hat{j}_p' \int_{|\hat{j}_p - \hat{l}|}^{\hat{j}_p + \hat{l}} d\hat{h} \sum_{s.p.} \frac{1}{(2\pi)^4} |\partial(\hat{j}'\hat{j}_p'\hat{l}'\hat{h}')/\partial(\bar{q}_j \bar{q}_{j_p} \bar{q}_l \bar{q}_h)|^{-1}$$

$$= \int_0^\infty d\hat{J} \int_0^\infty \tfrac{1}{2} d\hat{l}' \int_0^\infty \tfrac{1}{2} d\hat{j}_p' \int_{|\hat{j}_p - \hat{l}|}^{\hat{j}_p + \hat{l}} d\hat{h}\, \frac{8 \times 8}{(2\pi)^4} \sum_{s.p.} |\partial(\hat{j}'\hat{j}_p'\hat{l}'\hat{h}')/\partial(\bar{q}_j \bar{q}_{j_p} q_l \bar{q}_p)|^{-1}$$

$$= \int_0^\infty d\hat{J} \int_0^\pi d\bar{q}_l/\pi \int_0^\pi d\bar{q}_{j_p}/\pi \int_0^{2\pi} d\bar{q}_h/2\pi \left((4) \sum_{s.p.} \frac{1}{2\pi} |\partial\hat{j}'/\partial\bar{q}_j|^{-1} \right) \quad \text{after partial averaging}\,. \tag{A12}$$

The factor of (4) in Eq. (A12) serves as the symmetry number of Fitz and Marcus.[5]

One may verify by similar arguments that when the dipole–dipole potential is included, it is necessary to scan two octants of $\bar{q}_j$, $\bar{q}_{j_p}$, $\bar{q}_l$ space and that a symmetry number of 1 is appropriate for such a case. The intervals searched then are, respectively, $[0, 2\pi]$, $[0, \pi]$, and $[0, \pi]$.

[1]A. F. Turfa, D. E. Fitz, and R. A. Marcus, J. Chem. Phys. **67**, 4463 (1977), preceding article.
[2](a) P. W. Anderson, Phys. Rev. **76**, 647 (1949); (b) C. J. Tsao and B. Curnutte, J. Quant. Spectrosc. Radiat. Transfer **2**, 41 (1962).
[3](a) J. S. Murphy and J. E. Boggs, J. Chem. Phys. **47**, 691 (1967); (b) *ibid.* **47**, 4152 (1967); (c) *ibid.* **49**, 3333 (1968).
[4](a) G. Birnbaum, Adv. Chem. Phys. **12**, 487 (1967); (b) H. Rabitz, Ann. Rev. Phys. Chem. **25**, 155 (1974); (c) Krishnaji, J. Scient. Ind. Res. **32**, 168 (1973); (d) cf. D. E. Stogyrin and A. P. Stogryn, Mol. Phys. **11**, 371 (1966).
[5](a) D. E. Fitz and R. A. Marcus, J. Chem. Phys. **59**, 4380 (1973); (b) *ibid.* **62**, 3788 (1975).
[6](a) W. K. Liu and R. A. Marcus, J. Chem. Phys. **63**, 272 (1975); (b) *ibid.* **63**, 290 (1975); (c) W. K. Liu, Ph. D. dissertation, Univ. of Ill., Urbana IL, 1975.
[7](a) B. Th. Berendts and A. Dymanus, J. Chem. Phys. **48**, 1361 (1968); (b) *ibid.* **49**, 2632 (1968).
[8](a) J. C. McGurk, T. G. Schmalz, and W. H. Flygare, Adv. Chem. Phys. **25**, 1 (1974); (b) H. Mäder, J. Ekkers, W. E. Hoke, and W. H. Flygare, J. Chem. Phys. **62**, 4380 (1975); (c) W. E. Hoke, D. R. Bauer, J. Ekkers, and W. H. Flygare, J. Chem. Phys. **64**, 5276 (1976); (d) W. H. Flygare and T. G. Schmalz, Acc. Chem. Res. **9**, 385 (1976).
[9]R. G. Gordon, J. Chem. Phys. **44**, 3083 (1966).
[10](a) H. Margenau and N. R. Kestner, *Theory of Intermolecular Forces* (Pergamon, New York, 1971), 2nd ed; (b) J. O. Hirschfelder, C. F. Curtiss, and R. B. Bird, *Molecular Theory of Gases and Liquids* (Wiley, New York, 1967).
[11]R. A. Marcus, J. Chem. Phys. **54**, 3965 (1971).
[12](a) W. H. Miller, J. Chem. Phys. **54**, 5386 (1971); (b) Adv. Chem. Phys. **25**, 69 (1974).
[13]J. M. Hammersley and D. C. Handscomb, *Monte Carlo Methods* (Wiley, New York, 1964).
[14]Additional quantum mechanical interferences can occur as a result of orbiting and complex formation, but are "averaged out" in the present "partial averaging" and coarse-graining calculation.
[15]W. H. Flygare and R. C. Benson, Mol. Phys. **20**, 225 (1971).